Intramitochondrial Crystalline Inclusions in Nonalcoholic Steatohepatitis

Stephen H. Caldwell,[1] Luiz Antonio R. de Freitas,[2] Sang H. Park,[1,3] Maria Lucia V. Moreno,[2] Jan A. Redick,[4] Christine A. Davis,[4] Barbee J. Sisson,[4] James T. Patrie,[5] Helma Cotrim,[6] Curtis K. Argo,[1] and Abdullah Al-Osaimi[1]

Mitochondrial dysfunction is an important element in the pathogenesis of nonalcoholic steatohepatitis (NASH). Intramitochondrial crystals (IMCs) are a well-documented morphological abnormality seen on transmission electron microscopy in this disease. It has been suggested that IMCs consist of phospholipids, but their exact composition remain uncertain many years after their discovery. Micellar phase transitions of phospholipid bilayers is a well-known but little-studied phenomenon in living systems. Its presence in the mitochondria of NASH would offer significant insight into the disease with possible therapeutic implications. We postulated that intramitochondrial disturbances in NASH are sufficient to produce such transitions and that their detection in fresh biopsies would therefore be a dynamic process. To test this, we performed a blinded, prospective analysis of fresh liver biopsy samples immediately fixed under different conditions. Quantitative transmission electron microscopy morphometry, performed by systematically counting total mitochondria and IMCs within areas of uniform dimension, showed a stepwise decline in IMCs with cooler fixation temperature in each subject studied. Randomization testing (Monte Carlo resampling) confirmed that the detection of IMCs was strongly dependent on fixation temperature ($P < 0.0001$). *Conclusion:* These results indicate that the intramitochondrial crystals characteristic of NASH are highly dynamic and unstable structures. The findings offer the strongest support yet for their origin in micellar phase transitions. We speculate that such transitions result from microenvironmental changes within the mitochondria and carry therapeutic implications, especially in regard to dietary manipulations of mitochondrial lipid composition. (HEPATOLOGY 2009;49:1888-1895.)

Nonalcoholic steatohepatitis (NASH) is increasingly recognized as a form of obesity-related lipotoxicity. Intramitochondrial crystals (IMCs) are characteristic of human NASH and other types of steatohepatitis, such as alcohol-related liver injury, but are absent in common animal models of NASH.[1-4] Using conventional fixation, enlarged IMC-containing mitochondria are seen in adult and pediatric NASH in 5% to 15% of hepatocytes and 5% to 15% of the mitochondria within an affected cell (Fig. 1).[5,6] IMCs occur as parallel strands, each approximately 10 nm in diameter with 20 nm spaces between strands or, if cut cross-sectionally, as a two-dimensional lattice. The crystals occasionally appear to have continuity with the cristae, and a close association between the cristae and the crystals has been postulated.[7] These structures can be found throughout the hepatic lobule and correlate to oxidative injury.[8-10] Paradoxically, increased expression of IMCs is seen with histological improvement in thiazolidinedione-treated NASH patients.[11,12] Similar structures are observed in plant chloroplasts, where they represent inverted lipid membranes

Abbreviations: IMC, intramitochondrial crystal; MCRR, Monte Carlo resampling routine; NASH, nonalcoholic steatohepatitis; TEM, transmission electron microscopy.

From the [1]Division of GI/Hepatology, Department of Internal Medicine, the [4]Advanced Microscopy Center, and the [5]Department of Outcomes Medicine, University of Virginia, Charlottesville, VA; the [2]Oswaldo Cruz Foundation, Salvador-Bahia, Brazil; [3]GI/Hepatology, Hallym University Sacred Heart Hospital, Seoul, Korea; and the [6]Division of GI/Hepatology, Universidade Federal da Bahia, Salvador-Bahia, Brazil.

Received November 23, 2008; accepted January 13, 2009.

Supported by philanthropic gifts and grant CNPq-PAPES 400267/2006-3 from the Oswaldo Cruz Foundation.

Address reprint requests to: Stephen Caldwell, M.D., Division of GI/Hepatology, Department of Internal Medicine, Box 800708, University of Virginia Health System, Charlottesville, VA 22908-0708. E-mail: shc5c@virginia.edu; fax: 434-924-0491.

Published online in Wiley InterScience (www.interscience.wiley.com).

DOI 10.1002/hep.22851

Potential conflict of interest: Nothing to report.

Additional Supporting Information may be found in the online verison of this article.

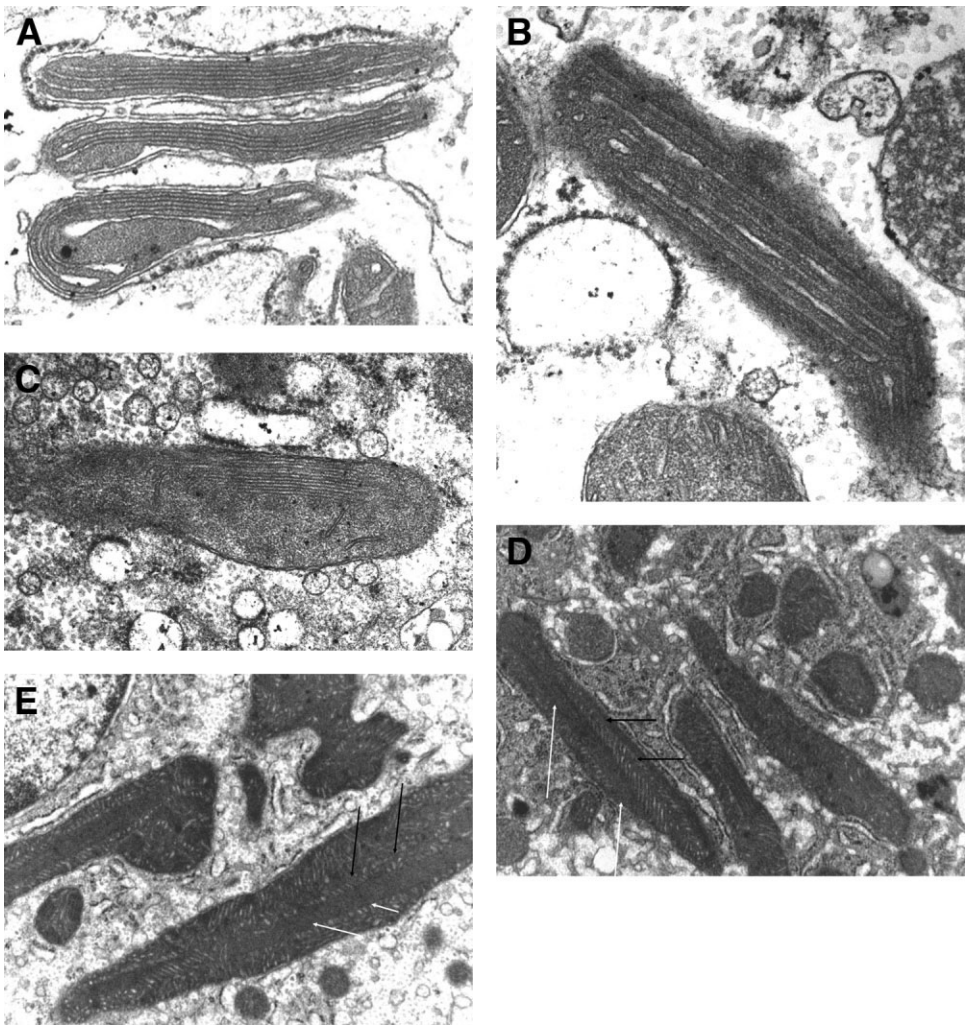

Fig. 1. TEM appearance of IMCs in human NASH. (A,B) Mitochondrial crystals in longitudinal form and their relationship to mitochondrial cristae. (C) The typical appearance of the crystals at higher magnification. (D,E) The appearance of mitochondria with crystals at the magnification used for quantitative morphometry (magnification ×10,000). Black arrows indicate linear crystals; white arrows indicate cristae.

as well as in bacteria exposed to oxidative stress where the structures consist of crystalline complexes of phospholipid, DNA, and ferritin-like substances.[13,14] In human alcohol-related liver disease, it has been suggested that the crystals are also primarily phospholipid.[15] Optical diffraction studies have further supported their origin in conformational changes of phospholipid micelles.[16]

The structure of the mitochondrial cristae is a dynamically regulated process that may be influenced by temperature and changes in lipid composition as well as expression of heat shock protein, cation content, and DNA content.[17-20] Based on factors that alter phase behavior of phospholipid bilayers and conditions within the mitochondria in NASH, we hypothesized that the fixation temperature of immediately prepared specimens from human NASH would influence detection of IMCs if their origin is in crystalline micellar phase transitions. Consistent with this hypothesis, our results indicate that fixation temperature strongly influences detection of these structures. These data offer the most convincing data yet available in support of their origin in micellar phase transitions. Because these structures are usually regarded as pathological in untreated NASH patients and because they are also influenced by lipid composition, our results have significant implications for therapeutic intervention.

Patients and Methods

The study subjects were patients with persistent abnormal serum aminotransferases undergoing diagnostic liver biopsy for suspected fatty liver disease based on clinical, laboratory, and imaging studies. Other liver diseases were excluded by serological and histological findings, which confirmed the diagnosis of NASH in all cases. None of the subjects was using thiazolidinediones or metformin

Table 1. Clinical Characteristics of Patients

Patient No.	Age/Sex	Body Mass Index (kg/m^2)	Fibrosis Stage*	NASH Activity Score†	Aspartate Aminotransferase	Alanine Aminotransferase	Major Risks
1	27/F	39	2	6	54	74	Obesity, hyperlipidemia
2	70/F	33	4	5	140	127	Obesity, hyperlipidemia
3	57/F	30	4	5	55	55	Obesity, diabetes mellitus
4	58/F	41	2	4	38	60	Obesity, hyperlipidemia

None of the patients was using thiazolidinedione, metformin, or statin-type medications within 3 months of undergoing biopsy.
*As described by Brunt et al.,[21] where stage 4 is cirrhosis.
†As described by Kleiner et al.[22]

within 3 months of the biopsy or had overt complications of portal hypertension. In all cases, routine processing of the core biopsy confirmed the presence of an active steatohepatitis via hematoxylin-eosin staining. The fibrosis stage (Masson trichrome staining) varied from stage 2 (portal fibrosis) to stage 4 (cirrhosis) according to Brunt et al.,[21] but all specimens including that with stage 4 fibrosis revealed an active steatohepatitis with ballooning and a NASH activity score of 4 or more according to Kleiner et al.[22] The clinical characteristics are summarized in Table 1.

At the time of the liver biopsy, three different segments (2 mm each) of liver tissue were separated from the core and each was immediately fixed (one segment each) at three different temperatures (37°C, 21°C, and 4°C) for 2 hours in a solution containing 4.0% (wt/vol) paraformaldehyde and 2.0% (wt/vol) glutaraldehyde in 0.1 M phosphate (pH 7.2) buffer for morphometric TEM analysis. In all cases the fixation solutions were brought to their respective temperatures 1 to 2 hours prior to the biopsy and maintained in thermometer-monitored baths for the warm and the cold temperatures or at ambient temperature (21°C) throughout the 2-hour fixation period. The specimens were then post-fixed in 1.0% osmium tetroxide, dehydrated in ethanol, and embedded in resin for sectioning. The resulting blocks were coded for blinded evaluation. Two half-micrometer sections ("thick sections") separated by 30 micrometers were taken from each block, providing two non-overlapping levels. The thick sections were stained with toluidine blue for examination via light microscopy to confirm adequacy of the samples. Two ultrathin sections (70–80 nm) were cut serial to the thick sections and placed, one section per grid, on 200 mesh copper grids. These were contrast-stained with lead citrate and uranyl acetate for examination via TEM. All processing of the specimens occurred in the Advanced Microscopy Facility at the University of Virginia by experienced electron microscopists (J. A. R., C. A. D., and B. J. S.).

Quantitative morphometry was performed by counting the total number of mitochondria and the total number of crystal-containing mitochondria from ×10,000 TEM negatives taken at the center of each of the counted grid spaces as described (Fig. 2).[12] Quantitative examination of the TEM grids was performed by experienced electron microscopists at the Oswaldo Cruz Foundation (L. A. R. F., M. L. V. M.) who were blinded to the temperature condition. Working in a raster from the upper left corner of the TEM grid, one 10K negative was taken from the center of each of the first 12 grid holes, which were fully covered by liver tissue. Grid holes only partially covered by liver tissue were omitted. Each high-resolution image represented 70 μm^2 at a magnification of ×10,000. The total area of liver examined at each temperature was as follows: 37°C; 13,440 μm^2 (16 grids, 192 grid areas); 21°C; 12,600 μm^2 (15 grids, 180 grid areas); 4°C; 13,160 μm^2 (16 grids, 188 grid areas). The study was approved by the University of Virginia Internal Review Board and by the Oswaldo Cruz Foundation. Biopsy material specifically intended for research was obtained under separate informed consent at the time of the biopsy for each patient.

In order to test the statistical significance of quantitative morphometry, randomization tests based on Monte Carlo resampling routines (MCRRs) were conducted to

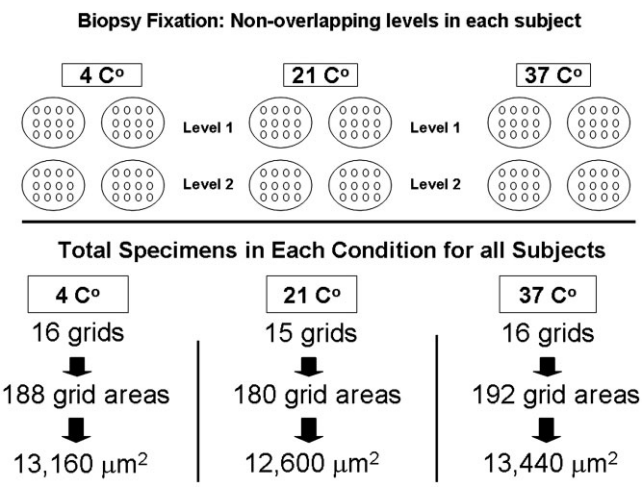

Fig. 2. Specimen preparation for quantitative TEM morphometry.

Table 2. Marginal Percentages for the Percentage of Mitochondria with Crystals Among All Grid Areas Examined (Mean % [SD])

Patient No.	Warm (37°C)	Ambient (21°C)	Cold (4°C)
1	35.3 (22.8)	15.1 (12.8)	6.8 (6.3)
2	20.7 (16.4)	7.8 (7.2)	2.3(2.2)
3	11.5 (10.2)	3.6 (3.5)	3.9 (3.8)
4	1.3 (1.3)	0.2 (0.2)	0 (0)
Overall	15.4 (13.0)	6.4 (5.9)	2.9 (2.8)

Distribution-Free Randomization Tests	No. of Random Shuffles	Global Test*	37°C versus 21°C	37°C versus 4°C	21°C versus 4°C
Patient 1	10,000	0.0001	0.0011	0.0001	0.0491
Patient 2	10,000	0.0001	0.0068	0.0001	0.0432
Patient 3	10,000	0.0004	0.0005	0.0028	0.8791
Patient 4	10,000	0.0255	0.0389	0.0262	0.7305
Overall†		<0.0001	<0.0001	<0.0001	0.1061

*Global test of the null hypothesis of no association between ICMs and liver biopsy specimen fixation temperature.

†*P* values computed via Fisher's exact test to combine independent *P* values.

compare, in global and pairwise fashion, the frequencies of IMCs under the three different specimen fixation temperature conditions.[23,24] Data analyses were conducted at both the within-subject level and at the group level using the Fisher's exact test to combine independent *P* values so that inference could be drawn at the group level.[25] The within-subject analyses were designed to determine whether the observed frequencies of IMCs under the three different fixation temperature conditions would be expected if there was no association between the frequency of IMCs and the specimen fixation temperature. The statistical package S-plus 7.0 (Insightful Corp., Seattle, WA) was used to conduct the randomization tests. The analytical details related to the MCRRs are presented in the accompanying appendix.

Results

Light microscopic examination of the routinely processed formalin-fixed biopsy cores confirmed the presence of histological steatohepatitis in all cases defined as >5% steatosis, cellular ballooning, inflammation, and fibrosis and scored according to Kleiner et al. (Table 1). After unblinding of the coded TEM specimens, there was no difference in the quality of tissue preservation or the total number of counted mitochondria between conditions of fixation or between patients. However, a stepwise decline was evident in each case in the percentage of mitochondria with crystals from warm to ambient to cool temperature fixation (Table 2 and Fig. 3). Overall, the percentage of crystal containing mitochondria was 15.4 ± 13.0 versus 6.4 ± 5.9 versus 2.9 ± 2.8 with warm (37°C), ambient (21°C), and cold (4°C) fixation, respectively. The randomization tests showed that the distribution of the percentage of mitochondria with crystals was strongly influenced by the fixation temperature for all patients ($P < 0.0001$). Examining each patient individually, the percentage of mitochondria with crystals remained strongly and significantly greater with warm (37°C C) fixation. These results are shown in Table 2 and Fig. 3.

Discussion

Alterations of mitochondrial form and function constitute a central element of the pathophysiology of fatty liver disease.[26-34] The mitochondria are a major source of reactive oxygen species and play a role in apoptosis signaling as a result of changes in permeability.[35-38] Structural changes have consistently included longitudinal or spherical swelling and the development of IMCs.[8,39] Based on optical diffraction studies, it has been suggested that IMCs represent crystalline phase transitions of the lamellar phospholipid bilayer.[16] This study shows that the ability to detect these structures in human NASH is strongly influenced by a single variable: fixation temperature. Thus, fixation at 37°C resulted in up to a five-fold increase in the presence of these structures, which indicates that IMCs are unstable and heat-dependent.

Because the specimens were immediately fixed under each of the temperature conditions within seconds of removal and only a single variable was applied, we believe that the structures represent phase transitions and that fixation at body temperature more accurately reflects the condition in vivo. Based on these results, it is likely that the frequency of IMCs has been greatly underestimated in past studies. On the other hand, we and others have previously shown that their detection is variable between individuals with fatty liver. Because other factors alter

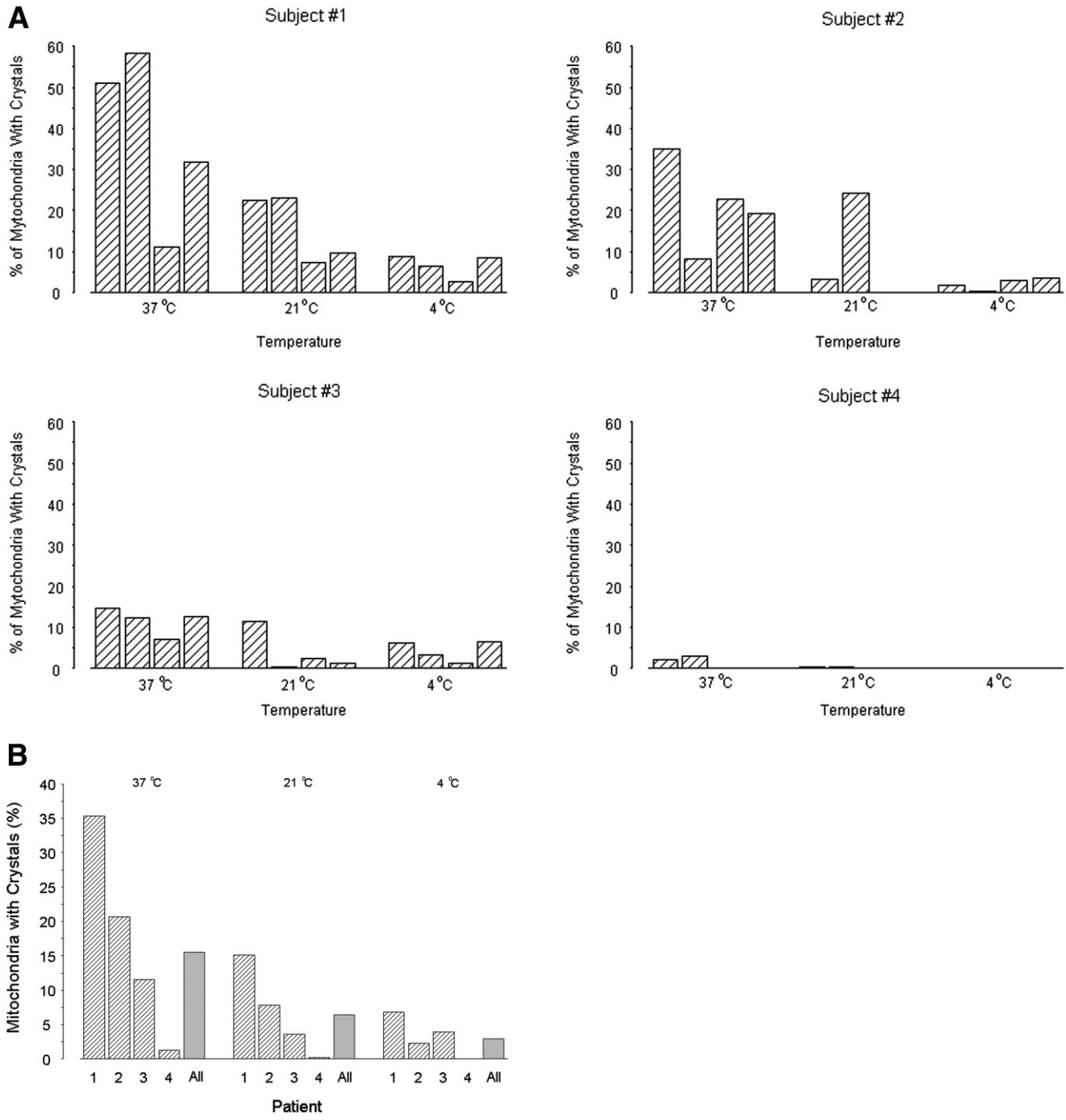

Fig. 3. (A) Percentage of mitochondria containing IMCs in each set of grids per condition per subject. (B) Percentage of mitochondria in each condition in each subject and combined (all).

expression of phase transitions (discussed below), some intersubject variation is expected. The fact that we observed the same pattern, decreasing with cooler temperature, in subjects with a higher frequency of IMCs and subjects with a lower frequency adds credence to the findings. These results have therapeutic implications, especially with regard to dietary lipid composition, because phase transitions also depend on lipid composition. However, whether these changes represent adaptive or entirely pathological changes and whether they are equally present in both obese and nonobese NASH patients remains unclear.

Phase transition of lipid bilayers represents the dynamic reversal of the polar head and hydrophobic fatty acid of phospholipids in relation to water and the resulting development of biocrystallization. Examples of phase

transitions in living systems include reversible crystalline lattices seen in light-deprived plant chloroplasts, where their morphology is also known to be influenced by associated membrane proteins.[40] Biocrystallization of phospholipids has also been observed in prokaryotes, where it is proposed to serve as a defensive mechanism that sequesters DNA from oxidative injury.[13,14,41] In the amoeba, oxidative stress has been reported to induce a reversible cubic structural transition in the mitochondria.[42,43] Different transitional phases of phospholipid bilayers are known, including lamellar, orthorhombic, and hexagonal phases. The phases can coexist in biological systems depending on a number of conditions, including temperature, fatty acid composition (saturated versus unsaturated), carbon chain length, ceramide content, lipid peroxides, heat shock protein expression, nonsequestered iron, deoxynucleic acid content, and membrane-bound protein content.[13,14,18-20,44-51] In human NASH, the mitochondria are similarly subject to conditions that influence expression of micellar bilayer phase transitions. These conditions include changes in lipid composition, changes in permeability and cation content, and the expression of uncoupling protein, which dissipates the energy of electron transport as heat.[52-62] Although the role of uncoupling protein in NASH is debated, changes in lipid composition together with changes in permeability may be sufficient to produce variably expressed phase transition in the mitochondrial cristae. Consistent with these findings, slight variations in the appearance of the crystals in relation to the cristae (Fig. 1) may represent different phospholipid transitional phases, which are known to coexist in isolated inner mitochondrial membranes depending on ambient conditions.[63]

Because of immediate fixation and the application of a single variable, our findings are consistent with the origin of IMCs in human NASH from phospholipid phase transitions. These results provide an important clue to the nature of these structures and give an indication of the degree of energy disequilibrium present in the steatotic liver. They also offer a potential therapeutic target, because lipid composition is subject to dietary lipid intake and strongly influences expression of the phase transitions. However, as with many of the secondary processes that follow oxidative stress, it is not yet clear whether these structures are entirely pathological or carry some adaptive advantage. Further work is needed to elucidate their role in NASH and other conditions associated with this abnormality, including alcohol-related liver disease and Wilson disease.

Appendix: Randomization Test

Each randomization test was based on 10,000 resampling routines. At each iteration of the MCRR, the fixation temperature conditions listed in the patient's dataset were randomly shuffled to produce a new dataset, which consisted of the same set of observational units (grid areas) and the same set of IMC frequencies as the original dataset, but with the data elements in the data column denoting the specimen fixation temperature condition (37°C, 21°C, and 4°C) shuffled in random order. Based on the random shuffled specimen fixation temperature conditions, one 3×2 cross-classification table and three 2×2 cross-classification tables were generated at each MCRR iteration. In accordance with the shuffled temperature condition assignments (37°C, 21°C, and 4°C), the 3×2 cross-classification table listed in separate rows of the 3×2 table the total number of mitochondria in which IMCs were detected and the total number of mitochondria in which IMCs were not detected. Similarly, in accordance with the shuffled temperature condition assignments, in pairwise fashion (37°C versus 21°C, 37°C versus 4°C, 21°C versus 4°C) the 2×2 cross-classification tables listed in separate rows of the 2×2 table the total number of mitochondria in which IMCs were detected and the total number of mitochondria in which IMCs were not detected.

For each of the 10,000 3×2 cross-classification tables, and for each of the 30,000 2×2 contingency tables, a chi-squared statistic was computed. In the case of the 3×2 cross-classification table, the chi-squared statistic was used as a relative measure of the degree of evidence against the global null hypothesis that the frequency of IMCs is unrelated to the specimen fixation temperature condition, and in the case of each of the 2×2 cross-classification tables, the chi-squared statistic was used as a relative measure of the degree of evidence against the null hypothesis that the percentage of mitochondria in which IMCs are detected is the same for the two biopsy specimen fixation temperatures (37°C and 21°C).

For the global hypothesis test as well as each pairwise null hypothesis test, the cumulative null distribution of the randomization test statistic was approximated by the cumulative frequency distribution of the 10,000 chi-squared statistics generated via the MCRRs. To globally test the null hypothesis that the IMC frequencies observed under the three different liver biopsy specimen temperature conditions occurred purely by chance, we calculated the total number of the 10,000 3×2 cross-classification tables that produced a chi-square statistic with magnitude greater than or equal to the magnitude of the chi-squared statistic produced by the 3×2 cross-classification table that contained the actual frequencies of IMCs under the three different fixation temperature conditions. Similarly, to test the null hypothesis that the IMC frequencies observed under two different liver biopsy

specimen temperature conditions occurred purely by chance, we calculated the total number of the 10,000 2 × 2 cross-classification tables that produced a chi-square statistic with magnitude greater than or equal to the magnitude of the chi-squared statistic produced by the 2 × 2 cross-classification table that contained the actual frequencies of IMCs under the two different fixation temperatures (37°C and 21°C).

By dividing each of the aforementioned totals by 10,000, the resulting proportions approximate the exact probability of observing a more extreme cross-classification table than the cross-classification table observed when the probability calculation considers all possible cross-classification tables of the same dimension that could be generated by the observed data. The decision rule for rejecting the global null hypothesis of no association between the frequency of IMCs and the specimen fixation temperature was based on a criterion of $P \leq 0.05$, and contingent on the global null hypothesis test being rejected, the decision rule for rejecting the individual pairwise null hypotheses was similarly based on a criterion of $P \leq 0.05$. The statistical package Splus 7.0 (Insightful Corp., Seattle, WA) was used to conduct the randomization tests.

Acknowledgment: The authors wish to acknowledge the invaluable insights of Carmen Mannella of the Wadsworth Center in Albany, NY, and Theo Wallman of the Institute of Cell Biology, ETH-Hönggerberg, Zürich.

References

1. Sternlieb I. Mitochondrial and fatty changes in hepatocytes of patients with Wilson's disease. Gastroenterology 1968;55:354-367.
2. Spycher MA, Ruttner JR. Kristalloide Einschlusse in menschlichen Lebermitochondrien. Virch Arch Abt B Zellpath 1968;1:211-221.
3. Kirsch R, Clarkson V, Shephard EG, Marais DA, Jaffer MA, Woodburne VE, et al. Rodent nutritional model of non-alcoholic steatohepatitis: Species, strain and sex difference studies. J Gastro and Hepatol 2003;18:1272-1282.
4. Chedid A, Mendenhall CL, Tosch T, Chen T, Rabin L, Garcia-Pont P, et al. Significance of megamitochondria in alcoholic liver disease. Gastroenterology 1986;90:1858-1864.
5. Caldwell SH, Swerdlow RH, Khan EM, Iezzoni JC, Hespenheide EE, Parks JK, et al. Mitochondrial abnormalities in nonalcoholic steatohepatitis. J Hepatol 1999;31:430-434.
6. Sobaniac-Lotowska ME, Lebensztejn DM. Ultrastructure of hepatocyte mitochondria in nonalcoholic steatohepatitis in pediatric patients: Usefulness of electron microscopy in the diagnosis of the disease. Am J Gastroenterol 2003;98:1664-1665
7. Haust MD. Crystalloid structures of hepatic mitochondria in children with heparin sulphate mucopolysaccharidosis (San filipo type). Exp Mol Pathol 1968;8:123-134.
8. Petersen P. Ultrastructure of periportal and centrilobular hepatocytes in human fatty liver of various aetiology. Acta Path Microbiol Scan (Sect A) 1977;85:421-427.
9. Sanyal AJ, Campbell-Sargent C, Mirshani F, Rizzo WB, Contos MJ, Sterling RK, et al. Nonalcoholic steatohepatitis: association of insulin resistance and mitochondrial abnormalities. Gastroenterology 2001;120:1183-1192.
10. Le TH, Caldwell SH, Redick JA, Sheppard BL, Davis CA, Arseneau K, et al. The lobular distribution of mitochondrial abnormalities in NASH. HEPATOLOGY 2004;39:1423-1429.
11. Caldwell SH, Hespenheide EE, Redick JA, Iezzoni JC, Battle EH, Sheppard Bl. A pilot study of a thiazolidinedione, troglitazone, in nonalcoholic steatohepatitis. Am J Gastroenterology 2001;96:519-525.
12. Caldwell SH, Patrie JT, Brunt EM, Redick JA, Davis CA, Park SH, et al. Increased mitochondrial crystalline inclusions after 48 weeks of rosiglitazone in human nonalcoholic steatohepatitis (NASH). HEPATOLOGY 2007;46:1101-1107.
13. Williams WP, Selstam E, Brain T. X-ray diffraction studies of the structural organisation of prolamellar bodies isolated from Zea mays. FEBS Lett 1998:422:252-254.
14. Wolf SG, Frenkiel D, Arad T, Finkel SE, Kolter R, Minsky A. DNA protection by stress-induced biocrystallization. Nature 1999:400:83-85.
15. Svoboda DJ, Manning RT. Chronic alcoholism with fatty metamorphosis of the liver. Mitochondrial alterations in hepatic cells. Am J Pathol 1964;44:645-662.
16. Sternlieb I, Berger JE. Optical diffraction studies of crystalline structures in electron micrographs. J Cell Biol 1969;43:448-455.
17. Mannella CA. Structure and dynamics of the mitochondrial inner membrane cristae. Biochim Biophys Acta 2006;1763:542-548.
18. Amar-Yuli I, Wachtel E, Shalev DE, Moshe H, Aserin A, Garti N. Thermally induced fluid reversed hexagonal (H_{II}) mesophase. J Phys Chem B 2007;111:13544-13553.
19. May ER, Kopelevich DI, Narang A. Coarse-grained molecular dynamics simulations of phase transitions in mixed lipid systems containing LPA, DOPA, and DOPE lipids. Biophys J 2008;94:878-90.
20. Tsvetkova NM, Horváth I, Török Z, Wolkers WF, Balogi Z, Shigapova N, et al. Small heat-shock proteins regulate membrane lipid polymorphism. Proc Natl Acad Sci U S A 2002:99:13504-13509.
21. Brunt EM, Janney CG, Di Bisceglie AM, Neuschwander-Tetri BA, Bacon BR. Nonalcoholic steatohepatitis: a proposal for grading and staging the histologic lesions. Am J Gastroenterol 1999;94:2467-2474.
22. Kleiner DE, Brunt EM, Van Natta ML, Behling C, Contos MJ, Cummings OW, et al. Nonalcoholic Steatohepatitis Clinical Research Network. Design and validation of a histologic scoring system for NAFLD. HEPATOLOGY 2005;41:1313-1321.
23. Edgington ES. Randomization Tests. 3rd ed. New York: Marcel Dekker, 1995.
24. Morgan BJT. Elements of Simulation. London: Chapman & Hall, 1984.
25. Elston RC. On Fisher's method of combining p-values. Biom J 1991;88:339-345.
26. Dianzani MU. The content of adenosine polyphosphates in fatty livers. Biochem J 1957;65:116-124.
27. Pessayre D, Fromenty B. NASH: a mitochondrial disease. J Hepatol 2005;42:928-940.
28. Caldwell SH, Chang CY, Nakamoto RK, Krugner-Higby L. Mitochondria in nonalcoholic fatty liver disease. Clin Liver Dis 2004;8:595-617.
29. Hoek JB, Cahill A, Pastorino JG. Alcohol and mitochondria: a dysfunctional relationship. Gastroenterology 2002;122:2049-2063.
30. Peralta C, Rosello-Catafau J. The future of fatty livers. J Hepatol 2004;41:149-151.
31. Kojima H, Sakurai S, Uemura M, Fukui H, Morimoto H, Tamagawa Y. Mitochondrial abnormality and oxidative stress in nonalcoholic steatohepatitis. Alcohol Clin Exp Res 2007;31:61S–66S.
32. Cortez-Pinto H, Chatham J, Chako VP, Arnold C, Rashid A, Diehl AM. Alterations in liver ATP homeostasis in human nonalcoholic steatohepatitis: a pilot study. JAMA 1999;282:1659-1664.
33. Pérez-Carreras M, Del Hoyo P, Martin MA, Rubio JC, Martín A, Castellano G, et al. Defective hepatic mitochondrial respiratory chain in patients with nonalcoholic steatohepatitis. HEPATOLOGY 2003;38:999-1007.
34. Raffaella C, Francesca B, Italia F, Marina P, Giovanna L, Sussana I. Alterations in hepatic mitochondrial compartment in a model of obesity and insulin resistance. Obesity 2008;16:958-964.

35. Li ZZ, Berk M, McIntyre TM, Gores GJ, Feldstein AE. The lysosomal-mitochondrial axis in free fatty acid-induced hepatic lipotoxicity. HEPATOLOGY 2008;47:1495-1503.
36. Wieckowska A, Zein NN, Yerian LM, Lopez AR, McCullough AJ, Feldstein AE. In vivo assessment of liver cell apoptosis as a novel biomarker of disease severity in nonalcoholic fatty liver disease. HEPATOLOGY 2006;44: 27-33.
37. Vander Heiden MG, Chandel NS, Williamson EK, Schumacker PT, Thompson CB. Bcl-xL regulates the membrane potential and volume homeostasis of mitochondria. Cell 1997;91:627-637.
38. Ramalho RM, Cortez-Pinto H, Castro RE, Sola S, Costa A, Moura MC, et al. Apoptosis and Bcl-2 expression in the livers of patients with steatohepatitis. Euro J Gastro Hepatol 2006;18:21-29.
39. Krahenbuhl S. Alterations in mitochondrial function and morphology in chronic liver disease: pathogenesis and potential for therapeutic intervention. Pharmac Ther 1993;60:1-38.
40. Williams WP, Selstam E, Brain T. X-ray diffraction studies of the structural organization of prolamellar bodies isolated from *Zea Mays.* FEBS Lett 1998;422:252-254.
41. Frazier BA, Pfeifer JD, Russell DG, Falk P, Olsén AN, Hammar M, et al. Paracrystalline inclusions of a novel ferritin containing nonheme iron, produced by the human gastric pathogen Helicobacter pylori: evidence for a third class of ferritins. J Bacteriol 1993:175:966-972.
42. Deng Y, Kohlwein SD, Mannella CA. Fasting induces cyanide-resistant respiration and oxidative stress in the amoeba Chaos carolinensis: implications for the cubic structural transition in mitochondrial membranes. Protoplasma 2002:219:160-167.
43. Almsherqi ZA, Kohlwein SD, Deng Y. Cubic membranes: a legend beyond the Flatland of cell membrane organization. J Cell Biol 2006;173:839-844.
44. Cambrea LR, Hovis JS. Formation of three-dimensional structures in supported lipid bilayers. Biophys J 2007;92:3587-3594.
45. Foht PJ, Tran QM, Lewis RNAH, McElhaney RN. Quantitation of the phase preference of the major lipids of the *Acholeplasma laidlawii* B membrane. Biochemistry 1995;34:13811-13817.
46. Li QT, Yeo MH, Tan BK. Lipid peroxidation in small and large phospholipid unilamellar vesicles induced by water-soluble free radical sources. Biochem Biophys Res Commun 2000:273:72-76.
47. Krishnaswamy R, Pabst G, Rappolt M, Raghunathan VA, Sood AK. Structure of DNA-CTAB-hexanol complexes. Phys Rev E Stat Nonlin Soft Matter Phys 2006;73:031904.
48. Shah J, Atienza JM, Rawlings AV, Shipley GG. Physical properties of ceramides: effect of fatty acid hydroxylation. J Lipid Res 1995;36:1945-1955.
49. de Kruijff B, Cullis PR. Cytochrome c specifically induces non-bilayer structures in cardiolipin-containing model membranes. Biochim Biophys Acta 1980;602:477-490.
50. Cullis PR, de Kruijff B, Hope MJ, Nayar R, Rietveld A, Verkleij AJ. Structural properties of phospholipids in the rat liver inner mitochondrial membrane. Biochim Biophys Acta 1980:600:625-635.
51. Bouwstra JA, Gooris GS, Dubbelaar FER, Ponec M. Phase behavior of lipid mixtures based on human ceramides: coexistence of crystalline and liquid phases. J Lipid Res 2001;42:1759-1770.
52. Puri P, Baillie RA, Wiest MM, Mirshahi F, Choudhury J, Cheung O, et al. A lipidomic analysis of nonalcoholic fatty liver disease. HEPATOLOGY 2007; 46:1081-1090.
53. McClain CJ, Barve S, Deaciuc I. Good fat/bad fat. HEPATOLOGY 2007;45: 1343-1346.
54. Horimoto M, Fulop P, Derdak Z, Wands JR, Baffy G. Uncoupling protein-2 deficiency promotes oxidant stress and delays liver regeneration in mice. HEPATOLOGY 2004;39:386-392.
55. Serviddio G, Bellanti F, Tamborra R, Rollo T, Capitanio N, Romano AD, et al. Uncoupling protein-2 (UCP2) induces mitochondrial proton leak and increases susceptibility of non-alcoholic steatohepatitis (NASH) liver to ischaemia-reperfusion injury. Gut 2008;57:957-965.
56. Fulop P, Derdak Z, Sheets A, Sabo E, Berthiaume EP, Resnick MB, et al. Lack of UCP2 reduces Fas-mediated liver injury in ob/ob mice and reveals importance of cell-specific UCP2 expression. HEPATOLOGY 2006;44:592-601.
57. Baffy G. Uncoupling protein-2 and non-alcoholic fatty liver disease. Front Biosci 2005;10:2082-2096.
58. Frazier AE, Kiu C, Stojanovski D, Hoogenraad NJ, Ryan MT. Mitochondrial morphology and distribution in mammalian cells. Biol Chem 2006; 387:1551-1558.
59. Scorrano L, Ashiya M, Buttle K, Weiler S, Oakes SA, Manella CA, et al. A distinct pathway remodels mitochondrial cristae and mobilizes cytochrome c during apoptosis. Dev Cell 2002;2:55-67.
60. Arnoult D, Grodet A, Lee YJ, Estaquier J, Blackstone C. Release of OPA1 during apoptosis participates in the rapid and complete release of cytochrome c and subsequent mitochondrial fragmentation. J Biol Chem 2005;280:35742-35750.
61. Chiappini F, Barrier A, Saffroy R, Domart M-C, Dagues N, Azoulay D, et al. Exploration of global gene expression in human liver steatosis by high-density oligonucleotide microarray. Lab Invest 2006;86:154-165.
62. Nomoto K, Tsuneyama K, Takahashi H, Murai Y, Takano Y. Cytoplasmic fine granular expression of 8-hydroxydeoxyguanosine reflects early mitochondrial oxidative DNA damage in nonalcoholic fatty liver disease. Appl Immunohistochem Mol Morphol 2008;16:71-75.
63. Cullis PR, de Kruijff B, Hope MJ, Nayar R, Rietveld A, Verkleij AJ. Structural properties of phospholipids in the rat liver inner mitochondrial membrane. Biochim Biophys Acta 1980;600:625-635.